Direct Observation of Imperfections in Semiconductor Crystals by Anomalous Transmission of X Rays

Cite as: Journal of Applied Physics **33**, 2760 (1962); https://doi.org/10.1063/1.1702544
Submitted: 19 February 1962 • Published Online: 11 June 2004

G. H. Schwuttke

Direct Observation of Imperfections in Semiconductor Crystals by Anomalous Transmission of X Rays

G. H. SCHWUTTKE
General Telephone & Electronics Laboratories, Inc., Bayside 60, New York
(Received February 19, 1962)

An experimental technique for the direct observation of imperfections in single crystals is described. It is based on the anomalous transmission effect of x rays observed in crystals of high perfection. The parallel beam method previously used only for the mapping of dislocations has been improved so that large area x-ray topographs are recorded. It can now be applied to the detection of impurities, segregation, and precipitation effects in semiconductor materials. Microsegregation of oxygen in silicon, precipitation of copper in silicon, and arsenic segregation in germanium were used to study the influence of segregation and precipitation on the anomalous transmission. Working conditions of x-ray diffraction microscopy are discussed, and it is shown that segregation phenomena produce typical impurity contrast which is reflection-dependent if the impurities are in solid solution. For precipitated impurities, this relation does not exist.

INTRODUCTION

X-RAY diffraction microscopy, as is now well known, is a powerful tool for the direct observation of imperfections in nearly perfect crystals. It can be performed in two different ways. One technique is based on the effect of primary extinction of x rays and the other applies the anomalous transmission effect. Both techniques have been used successfully for the mapping of dislocations.[1–6] Better results were obtained with the extinction technique.[5,6] Recently, the extinction technique was shown also to be very effective for the detection of partial and stair-rod dislocations in epitaxial silicon layers[7,8] and for the observation of diffusion-induced dislocations and their interaction in shallow diffused surface layers.[9] In addition, the extinction technique has been applied to the investigation of segregation and precipitation effects in semiconductor crystals.[10–12] The anomalous transmission technique as known is not yet widely used because of difficulties in the technique. In this paper we describe an improved anomalous transmission technique based on the parallel beam method[2,3] and its application to the direct observation of dislocations, segregation, and precipitation of impurities in semiconductor crystals.

ANOMALOUS TRANSMISSION

An extensive review article on the anomalous transmission of x rays has recently been published by Borrmann.[13] A brief résumé of the effect will be given here. Anomalous transmission of x rays occurs in nearly perfect crystals. It manifests itself as enhanced transmission if the crystal is set for Laue diffraction. The effect was discovered by Borrmann[14] and subsequently explained by von Laue[15] in terms of the reduction of normal photoelectric absorption due to the coincidence of electromagnetic field nodes and atom sites inside the crystal. The effect is best illustrated by the wavefield model.[16] According to this model, two standing waves are set up if a plane monochromatic x-ray wavetrain enters a slab of perfect crystal set for Laue diffraction.[17] The net energy flow is mostly along the atomic planes and the standing waves are perpendicular to the flow direction. For a simple lattice one of these standing waves (A) may have its nodal planes coinciding with the position of a family of lattice planes (hkl), while the other (N) has its notes halfway between. Assuming the atoms to be point absorbers, and the crystal to be thick

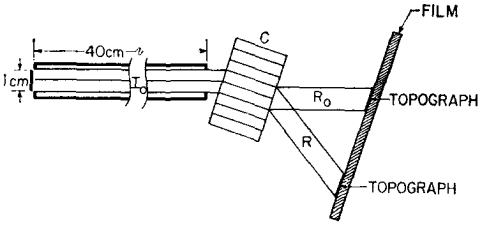

FIG. 1. Sketch of experimental arrangement.

[1] G. Borrmann, W. Hartwig, and H. Irmler, Z. Naturforsch. **13a**, 423 (1958).
[2] H. Barth and R. Hosemann, Z. Naturforsch. **13a**, 792 (1958).
[3] V. Gerold and F. Meier, Z. Physik **155**, 387 (1959).
[4] J. B. Newkirk, Phys. Rev. **110**, 1465 (1958).
[5] A. R. Lang, J. Appl. Phys. **29**, 527 (1958); **30**, 1748 (1959).
[6] G. H. Schwuttke, Semiconductor Symposium, ECS, Chicago, Illinois, May 1960, and Houston, Texas, October 1960.
[7] G. H. Schwuttke, Semiconductor Symposium, ECS, Detroit, Michigan, October 1961, 19th Annual Diffraction Conference, Pittsburgh, Pennsylvania, 1961; J. Appl. Phys. **33**, 1538 (1962).
[8] G. H. Schwuttke and V. Sils, Semiconductor Symposium, ECS, Los Angeles, May 1962.
[9] G. H. Schwuttke and H. J. Queisser, Bull. Am. Phys. Soc. **7**, 89 (1962); J. Appl. Phys. **33**, 1540 (1962).
[10] G. H. Schwuttke, J. Electrochem. Soc. **109**, 27 (1962).
[11] G. H. Schwuttke in *Direct Observations of Imperfections in Crystals*, edited by J. B. Newkirk and J. H. Wernick (Interscience Publishers, Inc., New York, 1962), p. 497.
[12] G. H. Schwuttke in *Ultrapurification of Semiconductor Materials*, edited by M. S. Brooks and J. K. Kennedy (The Macmillan Company, New York, 1962), p. 434.
[13] G. Borrmann in *Beitraege zur Physik* and *Chemie des 20 Jahrhunderts*, edited by Frisch, Paneth, Laves, and Rosbaud (Vieweg, Braunschweig, 1959), p. 262 (see also von Laue, reference 16).
[14] G. Borrmann, Physik. Z. **42**, 157 (1941); Z. Physik **127**, 297 (1950).
[15] M. von Laue, Acta Cryst. **2**, 106 (1949).
[16] M. von Laue, *Roentgenstrahlinterferenzen* (Akademische-Verlags Gesellschaft Frankfurt-am Main, 1960); also L. P. Hunter, J. Appl. Phys. **30**, 874 (1959).
[17] The wave patterns are comprised of four wavefields, 2 for each state of polarization.

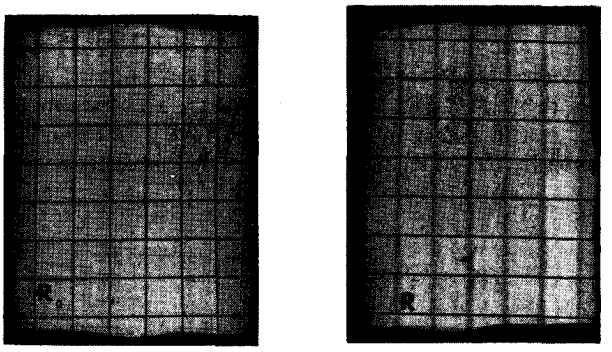

(a) (b)

FIG. 2. X-ray image of copper grid obtained by reflection from germanium crystal of zero dislocation density. Magnification 4×. (a) Position of grid between crystal and film; (b) position of grid between x-ray source and crystal.

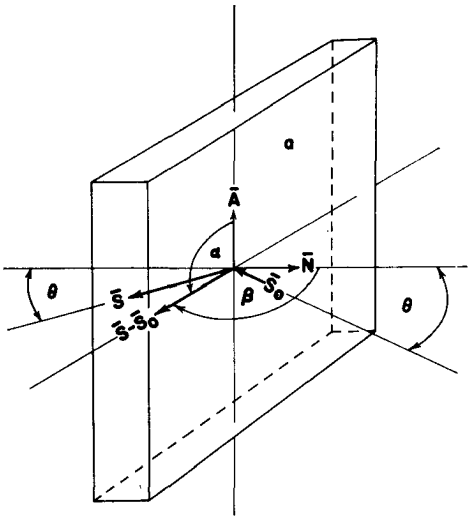

FIG. 3. Orientation of crystal wafer relative to x-ray beam for $\alpha=90°$, $\beta=90°$.

enough, the N wave soon becomes completely absorbed due to its strong interaction with the atoms, while the A wave passes with full intensity through the crystal independent of its thickness. On leaving the crystal the A wave decomposes equally into the transmitted beam R_0 and the diffracted beam R. Given real atoms and known structure factors, the A wave has a finite absorption coefficient. Its rate of attenuation depends also on the x-ray polarization. The x-ray beams leaving the crystal are therefore highly monochromatic, parallel, strongly polarized, and of surprisingly high intensity. However, the intensity depends critically on crystal perfection. Defects in the periodicity of the crystal

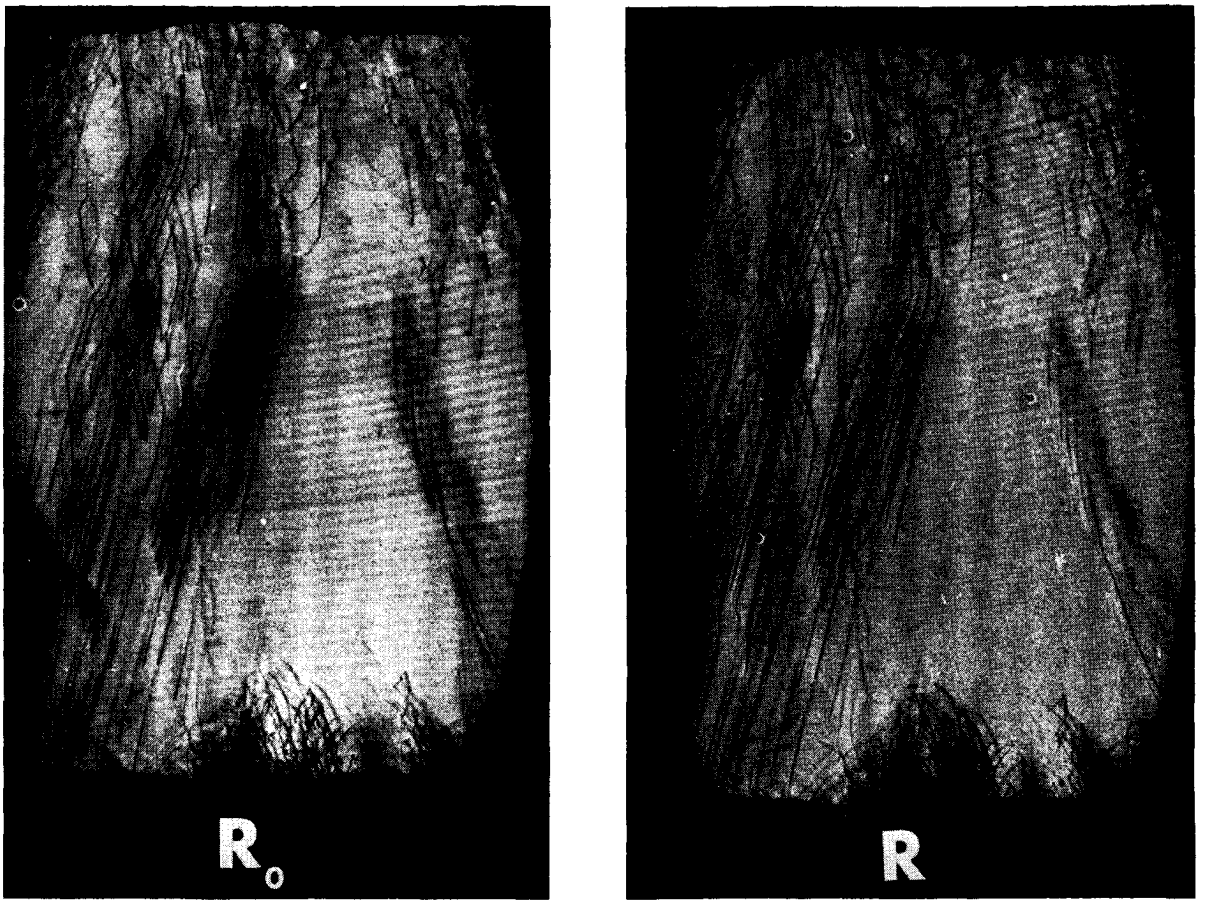

FIG. 4. R and R_0 image of germanium wafer showing dislocations; {110}-type reflection, $\alpha=90°$, $\beta=90°$. Magnification 8×.

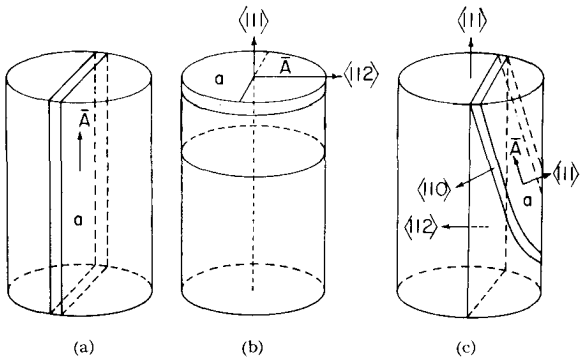

FIG. 5. Orientation of crystal wafers relative to bulk crystal.

reduce the intensity of the A wave. In effect, imperfections have been found to cast shadows in the field of the A wave just as obstacles do in the path of light rays.[1] Therefore, this effect can be used to observe imperfections in nearly perfect crystals.

EXPERIMENTAL TECHNIQUE

An experimental arrangement using the geometry of the parallel beam[2,3] is sketched in Fig. 1. The line focus lies in the plane of the drawing. B is a long collimator attached to the port of a standard x-ray unit. The crystal is mounted on a goniometer at position C. If the crystal is in a reflecting position, and the reflecting planes are at right angles to the crystal surface, the area of the portion of the crystal fulfilling Bragg's law is almost a rectangle, the width is approximately the extension of the line focus, and the height is determined by the geometry of the crystal slice or by a mask in front of the wafer. The film at position F placed parallel to the crystal surface records *two* identical topographs, one due to the direct beam R_0, and the other due to the diffracted beam R.

Because the R_0 and the R images are identical, it is sufficient to record one image only. Therefore, this experimental arrangement does not require the use of the specimen as its own filter as described in all previous arrangements as necessary for the elimination of white radiation which might pass through the crystal.[1–3] This can be done with a slit system which acts as a beam stop for R_0. Consequently, this arrangement makes possible the investigation of relatively thin specimens and extends the method to lighter elements such as silicon. In addition, the x-ray tube can be operated at higher voltage thus resulting in shorter exposure times.

In contrast to the extinction technique, use of highly monochromatic radiation is not required. For Cu $K\alpha_{12}$ the dispersion effect of the $K\alpha$ doublet is so small that it is negligible. Consequently, the resolution is excellent. The horizontal resolution in the image is essentially determined by the minimum separation of the $K\alpha$ doublet images on the film. If x denotes the distance between crystal and recording film, the horizontal separation of the $K\alpha$ doublet on the film can be expressed $R_H = x\Delta\theta/\cos^2\theta$, $\Delta\theta$ being the angular beam divergence due to the separation $\Delta\lambda$ of the peaks $K\alpha_1$ and $K\alpha_2$. Since the R_0 and R beams partially overlap, the distance x has a minimum value. This minimum value x_m depends on the effective source width ℓ and is given by the relation $x_m = \frac{1}{2}\ell\cot\theta$. For this distance the separation of the $K\alpha$ doublet on the film is a minimum. With the help of Bragg's law $\Delta\theta$ can be expressed as $\Delta\theta = (\Delta\lambda/\lambda)\tan\theta$, λ being the average wavelength of the doublet. The minimum separation of the $K\alpha$ peaks is thus obtained as $R_{\min} = (\ell/2\cos^2\theta)(\Delta\lambda/\lambda)$. For copper radiation and $\ell = 1$ cm, $R_{\min}$ is found to be approximately 13 $\mu/\cos^2\theta$. This value compares favorably with the 10-μ resolution of the extinction technique[5,10] and explains the picture quality which is comparable to the quality of extinction pictures.

The described experimental arrangement is capable of producing a nearly stigmatic image of an object placed in the path of the x-ray beam. Fig. 2(a) is the R_0 image of a grid, consisting of 50-μ-thick copper wires. The picture appears superimposed on the image of the reflecting Ge crystal which is of extremely high perfection. The grid was placed between crystal and film. For the grid placed between x-ray source and crystal, the image shown in Fig. 2(b) is obtained. In contrast to Fig. 2(a), the vertical wires in the image appear diffused. This is a direct verification of the energy spread in the crystal known as the Borrmann delta,[18] the action of

FIG. 6. R_0 image for high dislocation density in GaAs crystal; {110}-type reflection, $\alpha = 90°$, $\beta = 90°$. Magnification 7×.

[18] G. Borrmann, G. Hildebrandt, and H. Wagner, Z. Physik **142**, 406 (1955).

which is directly observable. Its influence on the visibility of dislocations is of some importance and will be pointed out later. Figure 2(b) was recorded by the R beam.

For the presentation of experimental results it is expedient to describe different orientations of the crystal wafer with respect to the x-ray beam by the angles α and β as defined in Fig. 3. Accordingly, the largest lateral crystal face of the wafer is a, the main axis of the wafer is $\bar{A}$ and the normal to the crystal face a is $\bar{N}$. If the direction of the incident beam is $\bar{S}_0$ and the direction of the diffracted beam $\bar{S}$, α is the angle between the diffraction vector $(\bar{S}-\bar{S}_0)$ and $\bar{A}$, and β is the angle between $(\bar{S}-\bar{S}_0)$ and $\bar{N}$. In our experiments the planes including $\bar{A}$ and $(\bar{S}-\bar{S}_0)$, respectively, $\bar{N}$ and $(\bar{S}-\bar{S}_0)$ are kept orthogonal to each other.

The experimental setup is such that the Bragg angle θ and the angle α are controlled with an accuracy of one minute of arc. The recording plate is placed parallel to the large lateral face a of the crystal. All x-ray micrographs presented in this paper were recorded with Cu radiation at 25 kV and 15 mA on Ilford nuclear plates emulsion G5, 50 μ thick. The exposure time varies between 5 to 10 h. The recorded crystal area is 1 cm^2. Areas as large as 2 cm^2 can be recorded for a different effective beam height.

The crystal wafers were cut approximately 1.2 mm thick from the bulk material. The large lateral face a is a low index face such as {111}, {110}, or {112}, and is oriented optically to an accuracy smaller than 30 min of arc.[19] After cutting and lapping, the wafers were etched to remove the surface layer; the crystal thickness is then approximately 1 mm. All micrographs presented are photographic negatives. The contrast on the nuclear plates is therefore reversed.

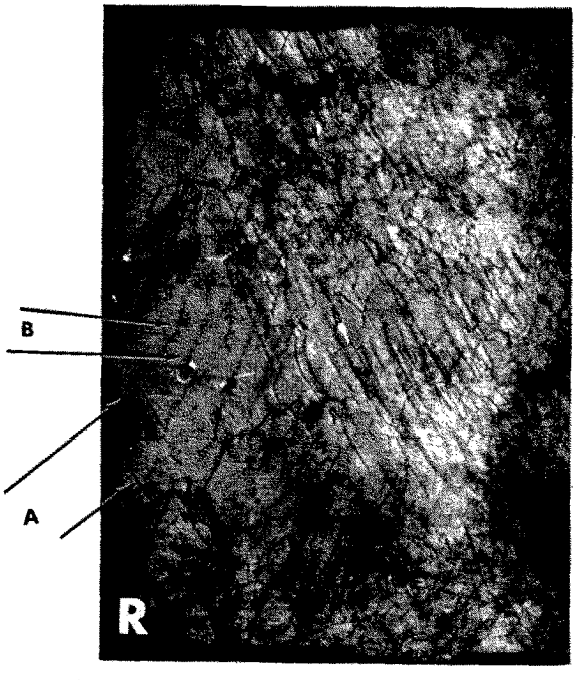

FIG. 7. Dislocations in Si wafer. {110}-type reflection, $\alpha=90°$, $\beta=90°$; R image. Magnification 6×.

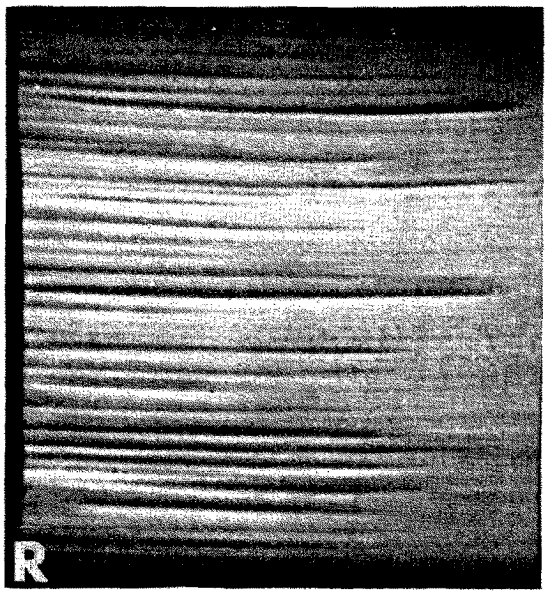

FIG. 8. Microsegregation of oxygen in silicon; {110}-type reflection, $\alpha=180°$, $\beta=90°$; R image. Magnification 7×.

DIFFRACTION MICROSCOPY OF DISLOCATIONS

The micrographs shown in Fig. 4 are the R and R_0 images of a Ge wafer. The slice was cut from a crystal grown in a ⟨111⟩ direction according to Fig. 5(a). The large lateral face is a {112} plane and contains the growth axis. The crystal is n type, arsenic doped. The R and R_0 images are completely identical as demanded by the theory of anomalous transmission. The dislocation lines are clearly visible as shadows because the anomalous transmitted wavefield is not propagated in their vicinity; it decomposes and normal absorption occurs.

The visibility of individual dislocations in the diffraction image depends on several factors. The dislocation density must be low enough so that individual dislocations are still recognizable in the image. This requires that the imperfect regions around and between the single lines do not overlap. The area between two lines must be sufficiently perfect to approximate the condition for anomalous transmission. This limits the maximum number of dislocations visible in an image. The photomicrograph shown in Fig. 6 is an anomalous transmission picture of a GaAs crystal. The crystal was grown in a ⟨111⟩ direction and the wafer was cut as indicated in Fig. 5(b). The dislocation density is approximately 10^6/cm^2. Crystals displaying a larger density cannot be investigated by this method.

The orientation of a dislocation line relative to the reflecting lattice plane exerts also a strong influence on its visibility. The line produces maximum contrast in

[19] G. H. Schwuttke, J. Electrochem. Soc. **106**, 315 (1959).

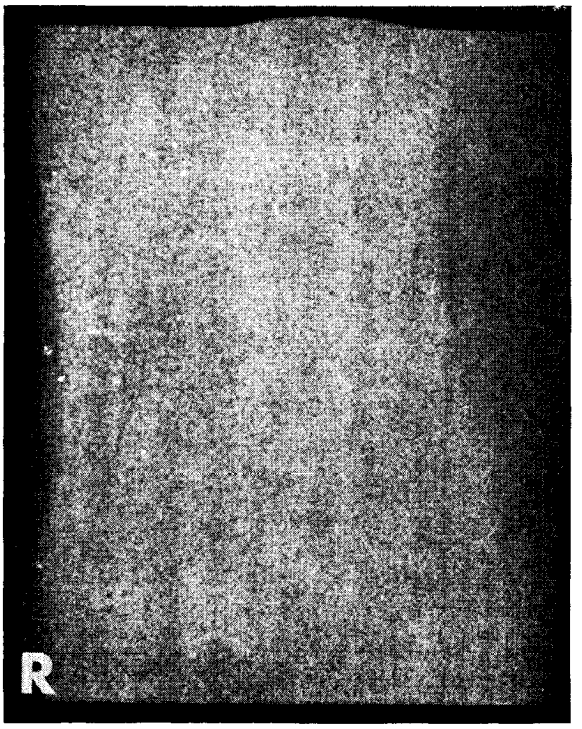

FIG. 9. Microsegregation of oxygen in silicon; {110}-type reflection, $\alpha=90°$, $\beta=90°$; R image. Magnification 7×.

the image if the Burgers vector is perpendicular to the reflecting lattice plane. The line is invisible if the Burgers vector lies in the reflecting plane. Therefore, Burgers vector determinations are possible.[5] The photomicrograph shown in Fig. 7 is an anomalous transmission picture of a silicon wafer cut according to Fig. 5(b). Many dislocations are visible with different contrast. The orientation of the lines marked A is such that they appear with maximum contrast, while lines marked B are practically invisible.

The influence of the Borrmann delta on the visibility of dislocations has already been mentioned. According to Borrmann *et al.*[18] the transport of radiation is not exactly parallel to the reflecting planes. The energy fans out forming a delta in the crystal. The influence of this fanning-out of radiation on the visibility of dislocations can be seen in Fig. 13(b). Dislocations not parallel to the surface plane of the wafer appear sharp where the beam enters the crystal, and fan-out toward the site where the beam leaves the crystal.

DIFFRACTION MICROSCOPY OF SEGREGATION AND PRECIPITATION

So far, x-ray diffraction microscopy by anomalous transmission has only been reported for the mapping of dislocations. Another important application, which extends the scope of the method considerably, is the detection of segregation and precipitation in the lattice. In general, one expects that any change in lattice periodicity will suppress the interaction between diffracted and incoming beams necessary for anomalous transmission. Thus, all localized imperfections will impede the propagation of the anomalous transmitted wavefield. The region of high strain surrounding areas of microsegregation and areas around precipitates in a perfect crystal lead to a breakdown of the anomalous transmission just as in the case of dislocation pipes. Thus certain reflections can be used to record these imperfections in the same way that dislocations are recorded.

SEGREGATION AND PRECIPITATION IN SILICON

Silicon crystals were selected for investigation of the influence of segregation and precipitation on the anomalous transmission of x rays. Oxygen segregation, silicon oxide and copper in silicon had been studied previously by the extinction technique.[10–12] As a direct result of these extensive studies, the influence of oxygen segregation and copper precipitation in silicon on the diffraction image is well understood and can be properly controlled. Samples for anomalous transmission studies were therefore pre-examined and selected by the extinction technique.

The photograph in Fig. 8 represents an anomalous transmission picture of a Si wafer of zero dislocation density containing microsegregation of oxygen. By evidence of the 9-μ absorption method,[20] the oxygen concentration is approximately 3×10^{17} atoms/cc. The variation in oxygen concentration along the growth axis

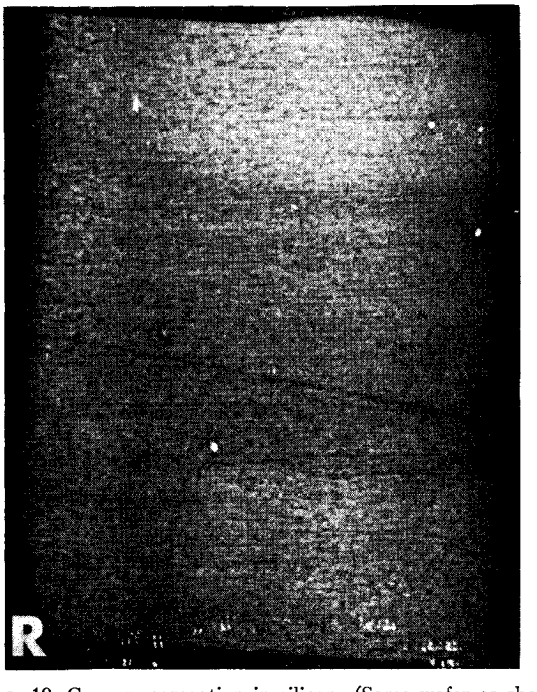

FIG. 10. Copper segregation in silicon. (Same wafer as shown in Fig. 9); {110}-type reflection, $\alpha=90°$, $\beta=90°$; R image. Magnification 7×.

[20] W. Kaiser, P. H. Keck, and C. F. Lange, Phys. Rev. **101**, 1264 (1956).

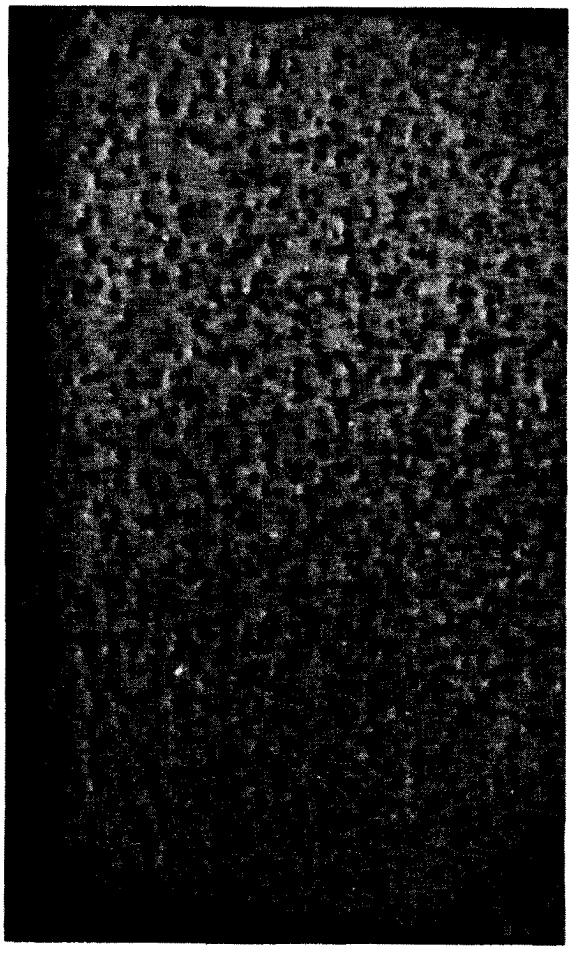

FIG. 11. Copper precipitation in silicon crystal of zero dislocation density; {110}-type reflection, $\alpha=90°$, $\beta=90°$; R image, Magnification 8×.

due to segregation is approximately 5×10^{16} atoms/cc. No precipitation of silicon oxide is present as measured by infrared light scattering.[21] The crystal was grown in a ⟨110⟩ direction and the wafer was cut according to Fig. 5(a). The large lateral face is an {001}. The image was recorded with the R beam by a {110}-type reflection perpendicular to the growth direction. Figure 9 is a diffraction image of the same crystal wafer, but this time recorded by a {110}-type reflection parallel to the growth axis.

The anomalous transmission measurements are analogous to the extinction contrast results.[10–12] For the reflection perpendicular to the growth axis the segregation stripes appear with maximum contrast, while for the diffracting plane parallel to the growth axis the segregation stripes are not visible. This result is quite important because the reflection-dependence is indicative of the absence of a second phase. If precipitation in the segregation areas exists, the segregation stripes are visible in all reflections including the one parallel to the growth axis. This will be shown for copper precipitates. If copper is diffused into silicon containing oxygen segregation, the copper segregates in the areas of high oxygen concentration and precipitates there after quenching.[22] The micrograph presented in Fig. 10 is that of the wafer shown in Fig. 9 but after copper diffusion at 850°C and subsequent quenching to room temperature. The solubility of copper in silicon at 850°C is approximately 5×10^{16} atoms/cc.[23] The copper has precipitated consequently the striations are now visible in the image which was recorded by the same reflection as that in Fig. 9.

The influence of random precipitation of copper on the anomalous transmission can be seen in Fig. 11. This micrograph is the x-ray image of a silicon crystal of zero dislocation density containing copper precipitates. The crystal was cut according to Fig. 5(b). Copper was diffused at 900°C, and the sample was subsequently quenched to room temperature to achieve precipitation. The solubility of copper in silicon at 900°C is approximately 10^{17} atoms/cc.[23] Figure 12 is the same picture

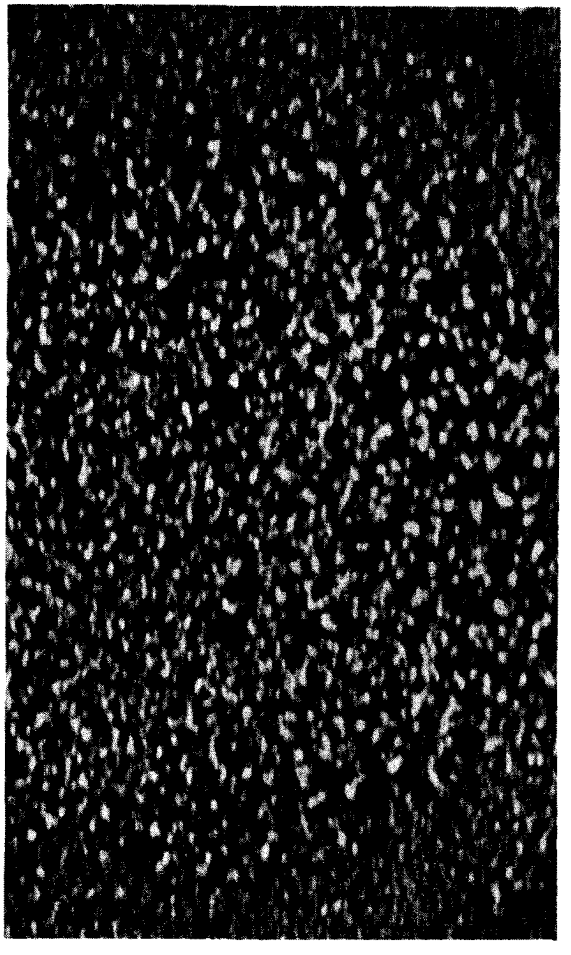

FIG. 12. Extinction picture of wafer shown in Fig. 11; {110}-type reflection, $\alpha=90°$, $\beta=90°$. Magnification 8×.

[21] G. H. Schwuttke, O. Weinreich, and P. H. Keck, J. Electrochem. Soc. **105**, 706 (1958).

[22] G. H. Schwuttke, J. Electrochem. Soc. **108**, 163 (1961).

[23] J. D. Struthers, J. Appl. Phys. **97**, 1560 (1956).

obtained by extinction contrast shown here for comparison. Both pictures clearly show random precipitation of copper. It is also of interest to note that the contrast in Fig. 11 is the reverse of that in Fig. 12.

Segregation and Precipitation in Highly Doped Germanium

With the influence of segregation and precipitation effects on the anomalous transmission of x rays established, it is now possible to detect precipitation and segregation in single crystals by the anomalous transmission technique. This will be shown for germanium crystals heavily doped with arsenic. This material is of considerable interest because of its use in tunnel diodes. Recently, evidence has been presented showing that at high dopant concentrations large fractions of arsenic remain electrically inactive. Measurements seem to indicate that the electrically inactive arsenic probably precipitated on cooling the crystal after growth. Striking resistivity changes have also been reported in heavily doped *n*-type germanium samples, indicating the presence of small areas that differ considerably in dopant concentration.[24] The diffraction micrographs of Fig. 13 show a germanium wafer cut from a crystal grown in a syringe-type crystal puller by the Czochralski technique.[25] The crystal is heavily arsenic doped, resistivity approximately 0.0009 Ω-cm. The wafer was cut according to Fig. 5(c). Both pictures were recorded {110}-type reflections. The reflecting plane in Fig. 13(a) makes an angle of 60° with the long side of the crystal, which contains the growth axis, while the reflecting plane in Fig. 13(b) is parallel to the growth axis. Several interesting diffraction phenomena, found to be typical for this material, can be noted. Most pronounced are the striations across the wafer which are present in both figures, but only faintly visible in Fig. 13(b) and the black patches labeled A. On the nuclear plate the striations are also faint but much clearer, some contrast has been lost in reproduction. The striations indicate a variation of dopant concentration along the growth axis. The spacing of the striations has been found to be equal to the distance the crystal grows during one rotation. Periodic variations in impurity concentrations

(a) (b)

FIG. 13. Heavily-doped germanium crystal {110}-type reflections. Magnification 8×. (a) $\alpha=150°$, $\beta=90°$; R image; (b) $\alpha=90°$, $\beta=90°$; R_0 image.

[24] W. G. Spitzer, F. A. Trumbore, and R. A. Logan, J. Appl. Phys. **32**, 1822 (1961).
[25] The crystal was grown by K. M. Arnold, General Telephone & Electronics Laboratories, Inc.

(striations) along the growth axis are typical for semiconductor single crystals pulled from the melt by the Czochralski technique. The striations are attributed to the fact that the temperature distribution at the solid-liquid interface is not radially symmetric.[26] The results of Fig. 13 are strong evidence that some precipitation of arsenic must have occurred during cooling after growth. This conclusion is substantiated by the micrograph of Fig. 4 recorded by the same reflection as the one in Fig. 13(b); it represents a wafer cut from the same bulk crystal but from a different section. The segregation stripes are stronger in this image, therefore more arsenic must have precipitated in this section.

The black patches at positions A in Fig. 13 are areas where the anomalous transmission is strongly reduced. By comparing 13(a) and 13(b) it is found that the contrast at A is reflection-dependent. The most likely explanation for these areas is that they represent regions of enhanced arsenic concentration. Some precipitated arsenic must also be present, otherwise the reflection dependence would be stronger.

DISCUSSION

In discussing the best working conditions for x-ray diffraction microscopy, it is very useful to compare the anomalous transmission against the extinction technique. Results obtained by the two methods are essentially identical, but in general one technique cannot be substituted for the other because the conditions for optimum contrast in the image are not the same. The anomalous transmission technique requires that for good contrast the product of the linear absorption coefficient $\mu(\text{cm}^{-1})$ and slice thickness $t(\text{cm})$ is large, preferably larger than 20; for the extinction technique this product should be smaller than unity. Therefore soft radiation such as copper is used for the anomalous transmission technique and hard penetrating radiation such as molybdenum for the extinction technique. The imperfection contrast is also typical for each technique. This can be seen in Figs. 11 and 12. Figure 11 shows absorption contrast in which the imperfections are visible as shadows; Fig. 12 shows diffraction contrast in which the imperfections are visible by enhanced contrast. The achievable image resolution is approximately equal for both methods. The advantage of the anomalous transmission technique is the simplicity of the setup that has been described here. In this form it is a stationary technique. Crystal areas up to 2 cm^2 can be recorded without moving the crystal. The extinction technique requires scanning, but larger areas can be recorded. The experimental arrangement of the extinction technique could also be used for anomalous transmission measurements, but this would defeat the purpose of the setup described, and require extremely long exposure times. The ratio of the required exposure times for the two arrangements if used in anomalous transmission is approximately equal to the ratio of the effective source dimensions in the horizontal plane, which is about 10, if the same x-ray tube is used in both arrangements.

The intensity conditions are much more favorable for extinction contrast than for anomalous transmission. The required exposure time is, therefore, longer for anomalous transmission measurements; if equal areas are recorded, the scanning extinction technique requires approximately one-half the exposure time necessary for the stationary anomalous transmission technique.

In conclusion it should be pointed out that both techniques are nondestructive and noncompetitive; rather, they are complementary, and together make x-ray diffraction microscopy a remarkably effective tool for the direct observation of imperfections in nearly perfect crystals.

[26] E. Billig, Proc. Roy. Soc. (London) **229**, 346 (1955); also P. R. Camp, J. Appl. Phys. **25**, 459 (1954).

ACKNOWLEDGMENTS

The author is indebted to E. Jungbluth and R. Modena for their help in performing the measurements.

The research reported in this paper was sponsored by the U. S. Air Force Cambridge Research Laboratories under Contract AF 19(604)7313.